Cancer Cell
Article

Small Molecule Inhibitors of Aurora-A Induce Proteasomal Degradation of N-Myc in Childhood Neuroblastoma

Markus Brockmann,[1,8] Evon Poon,[2,8] Teeara Berry,[2] Anne Carstensen,[1] Hedwig E. Deubzer,[5] Lukas Rycak,[6] Yann Jamin,[5] Khin Thway,[4] Simon P. Robinson,[3] Frederik Roels,[7] Olaf Witt,[5] Matthias Fischer,[7] Louis Chesler,[2,9,*] and Martin Eilers[1,9,*]
[1]Comprehensive Cancer Center Mainfranken and Theodor Boveri Institute, Biocenter, University of Würzburg, Am Hubland, 97074 Würzburg, Germany
[2]Division of Clinical Studies and Cancer Therapeutics
[3]Division of Radiotherapy and Imaging
[4]Division of Pathology
The Institute of Cancer Research, The Royal Marsden NHS Trust, 15 Cotswold Road Belmont, Sutton, Surrey SM2 5NG, UK
[5]CCU Pediatric Oncology, DKFZ and Department of Pediatrics 3, University Hospital Heidelberg, Germany, Im Neuenheimer Feld 280, 69120 Heidelberg, Germany
[6]Institute of Molecular Biology and Tumor Research (IMT), Emil-Mannkopff-Str. 2, 35037 Marburg, Germany
[7]University Children's Hospital of Cologne and Cologne Center for Molecular Medicine (CMMC), University of Cologne, Kerpener Str. 62, 50924 Cologne, Germany
[8]These authors contributed equally to this work and are co-first authors
[9]These authors contributed equally to this work and are co-senior authors
*Correspondence: louis.chesler@icr.ac.uk (L.C.), martin.eilers@biozentrum.uni-wuerzburg.de (M.E.)
http://dx.doi.org/10.1016/j.ccr.2013.05.005

SUMMARY

Amplification of *MYCN* is a driver mutation in a subset of human neuroendocrine tumors, including neuroblastoma. No small molecules that target N-Myc, the protein encoded by *MYCN*, are clinically available. N-Myc forms a complex with the Aurora-A kinase, which protects N-Myc from proteasomal degradation. Although stabilization of N-Myc does not require the catalytic activity of Aurora-A, we show here that two Aurora-A inhibitors, MLN8054 and MLN8237, disrupt the Aurora-A/N-Myc complex and promote degradation of N-Myc mediated by the Fbxw7 ubiquitin ligase. Disruption of the Aurora-A/N-Myc complex inhibits N-Myc-dependent transcription, correlating with tumor regression and prolonged survival in a mouse model of *MYCN*-driven neuroblastoma. We conclude that Aurora-A is an accessible target that makes destabilization of N-Myc a viable therapeutic strategy.

INTRODUCTION

Deregulated expression of *MYC*, *MYCL*, or *MYCN*, which encode c-Myc, L-Myc, and N-Myc, respectively, contributes to the genesis of multiple human tumors. Amplification of *MYCN* is found in neuroendocrine tumors, including neuroblastoma, small cell lung carcinoma, and neuroendocrine prostate cancer (Beltran et al., 2011; Brodeur et al., 1984; Kim et al., 2006). Deregulated expression of *MYCN* also occurs in tumors lacking *MYCN* amplification, since *MYCN* is downstream of several oncogenic signal transduction pathways (Valentijn et al., 2012). Paradigmatic examples are mutations in the sonic hedgehog pathway that drive a subset of human medulloblastomas and lead to constitutively elevated expression of *MYCN* (Hatton et al., 2006; Kawauchi et al., 2012).

Similar to c-Myc, the N-Myc protein is a DNA binding helix-loop-helix/leucine zipper protein that forms an obligate heterodimer with a partner protein termed Max (Wenzel et al., 1991). Both the interface between the two subunits and the interface between the dimer and the DNA sequences it bound are

Significance

Multiple previous studies suggest that targeting members of the Myc family of oncoproteins will have significant therapeutic benefit in human tumors. Deregulated expression of N-Myc, one of the three Myc family members, is prevalent in both pediatric and adult neuroendocrine tumors. We show here that it is possible to target N-Myc indirectly using small molecules that disrupt the interaction between N-Myc and the Aurora-A kinase, which is critical for stabilizing N-Myc. In a mouse model of neuroblastoma, such inhibitors induce differentiation and senescence in tumors and achieve significant therapeutic benefit.

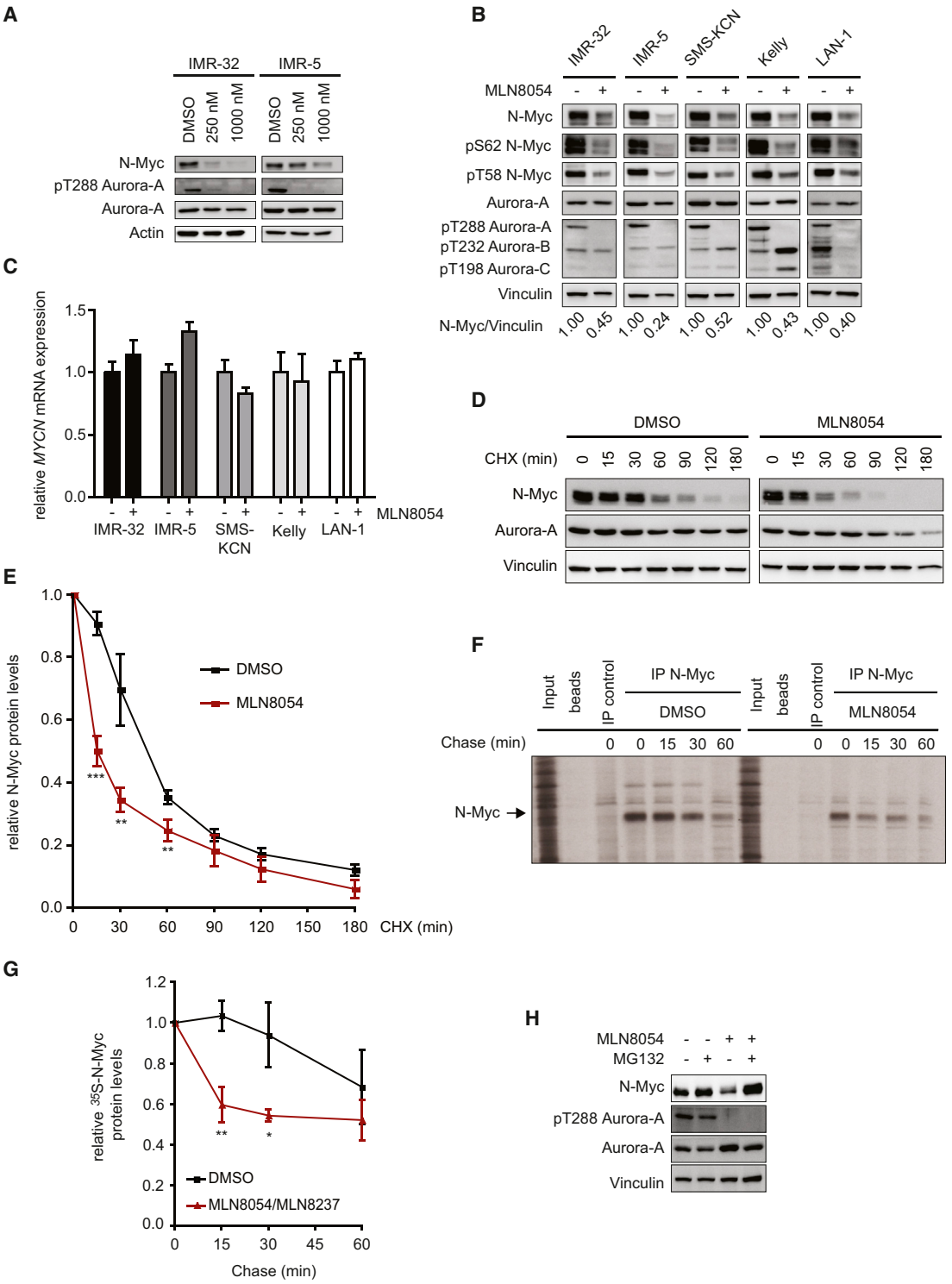

Figure 1. Effect of MLN8054 on N-Myc Expression and Stability in *MYCN*-Amplified Neuroblastoma Cell Lines

(A) The panels show immunoblots of IMR-32 and IMR-5 cells treated for 48 hr with the indicated concentrations of MLN8054 or solvent control (0.1% v/v DMSO). The results are representative of four independent experiments (n = 4; unless otherwise indicated, n indicates the number of independent experiments in the following legends).

(B) The panels show representative immunoblots of five *MYCN*-amplified neuroblastoma cell lines upon treatment with MLN8054 (1,000 nM; 48 hr) or solvent control (n = 3). Ratios of N-Myc to vinculin are indicated below the panel.

(C) The graphs show quantitative RT-PCR assays of *MYCN* mRNA levels relative to β2-microglobulin and *RPS14* as control. RNA was isolated from the indicated cell lines treated with MLN8054 (1,000 nM, 24 hr) or solvent control. Error bars indicate mean +SD of triplicate technical assays (n = 2).

(legend continued on next page)

extensive, and currently no small molecule inhibitors that target the heterodimeric complex are clinically available. Since N-Myc binds to a large set of target genes, defining critical oncogenic effector pathways that can be targeted for therapeutic intervention is also difficult (Chen et al., 2008).

Like c-Myc, N-Myc is degraded via the ubiquitin-proteasome system. One ubiquitin ligase that targets N-Myc for proteasomal degradation is Fbxw7, which recognizes N-Myc upon phosphorylation at both S62 and T58 (Sjostrom et al., 2005). The mitotic kinase cyclin B/CDK1 phosphorylates S62, thereby priming phosphorylation at T58 by GSK3β. As a result, N-Myc is specifically degraded during mitosis (Sjostrom et al., 2005). This mechanism is thought to enable cell-cycle exit and differentiation of neural progenitor cells and to "reset" N-Myc levels before the start of the next cell cycle.

MYCN-amplified neuroblastoma cells express elevated levels of Aurora-A, a kinase that is expressed and active during G2 and mitosis (Marumoto et al., 2005; Otto et al., 2009). Aurora-A associates with N-Myc and prevents Fbxw7-mediated proteasomal degradation of N-Myc. *MYCN*-amplified neuroblastoma cells depend on high levels of Aurora-A expression for maintaining N-Myc function (Otto et al., 2009). Similarly, Aurora-A and N-Myc bind each other and together drive an oncogenic gene expression program in neuroendocrine prostate tumors (Beltran et al., 2011). Neither complex formation with nor stabilization of N-Myc requires the catalytic activity of Aurora-A. As a result, several Aurora kinase inhibitors have no discernible effect on N-Myc turnover (Otto et al., 2009). However, complex formation requires the kinase domain of Aurora-A, and some of the available inhibitors of Aurora-A induce an unusually distorted conformation of this domain, in which the transactivation loop [featuring an Asp(D)-Phe(F)-Gly(G) sequence] adopts an apparently nonphysiological conformation ("DFG-up") (Dodson et al., 2010; Sloane et al., 2010). The goal of this study was to test the effect of such inhibitors on N-Myc expression and stability and determine their therapeutic potential in a mouse model of *MYCN*-driven neuroblastoma.

RESULTS

We showed previously that Aurora-A forms a complex with N-Myc in *MYCN*-amplified neuroblastoma cells, which protects N-Myc from proteasomal degradation in mitosis (Otto et al., 2009). This activity was specific for Aurora-A, since neither enhanced expression of Aurora-B nor small interfering RNA (siRNA)-mediated depletion of Aurora-B affected N-Myc protein levels (Figures S1A and S1B available online). Stabilization of N-Myc does not require the catalytic activity of Aurora-A (Otto et al., 2009). However, recent crystallographic work shows that the Aurora-A-specific inhibitor MLN8054 (Manfredi et al., 2007) induces a DFG-up conformation, in which multiple residues have an altered position relative to ATP-bound Aurora-A, raising the possibility that MLN8054 disrupts the Aurora-A/N-Myc complex (Dodson et al., 2010; Sloane et al., 2010). This result prompted us to test whether MLN8054 might affect N-Myc stability. We therefore treated *MYCN*-amplified neuroblastoma IMR-32 and IMR-5 cells with increasing concentrations of MLN8054 (Manfredi et al., 2007). Treatment with MLN8054 abolished autophosphorylation of Aurora-A at Thr288 (T288) and caused a concentration-dependent decrease in N-Myc protein levels (Figure 1A). Treatment of three additional *MYCN*-amplified neuroblastoma lines also decreased N-Myc protein levels (Figures 1B and S1C). In all cell lines, the decrease in N-Myc levels was apparent after 24 hr of treatment (Figure S1C). In four of five lines, there was a further decrease between 24 and 48 hr (compare Figure 1B, 48 hr, with Figure S1C, 24 hr). MLN8054 abolished autophosphorylation of Aurora-A at T288 but had no consistent effects on the autophosphorylation of Aurora-B and Aurora-C, consistent with it being a specific Aurora-A inhibitor at the concentrations used here (Figures 1B and S1C). Furthermore, MLN8054 did not significantly alter the expression of GSK3β and the phosphorylation of GSK3β at Ser9 (Figures S1C and S1G). This observation is consistent with the lack of effect of either overexpression or siRNA-mediated depletion of Aurora-A on GSK3β phosphorylation and argues that Aurora-A does not affect N-Myc stability via effects on GSK3β or its upstream regulators (Figures S1D and S1E) (Faisal et al., 2011). Similarly, incubation of *MYCN*-amplified neuroblastoma cell lines with the clinical lead compound MLN8237, which is structurally closely related to MLN8054, decreased N-Myc protein levels, arguing that this is not an off-target effect of MLN8054 (Figure S1F) (Manfredi et al., 2011).

Treatment with MLN8054 or MLN8237 had little effect on *MYCN* messenger RNA (mRNA) levels and decreased levels of N-Myc expressed from a heterologous promoter in SH-EP neuroblastoma cells, demonstrating that both compounds decrease N-Myc levels via a posttranscriptional mechanism (Figures 1C, S1G, and S1H). In normal neuronal progenitors, N-Myc is degraded in G2/M, since degradation is initiated by phosphorylation by cyclin B/CDK1 (Sjostrom et al., 2005). Fluorescence-activated cell sorting (FACS) experiments showed that approximately 70% of IMR-32 cells accumulated in G2/M upon treatment with MLN8054 or MLN8237 for 24 hr (Figure S1F). Under these conditions, measurements of N-Myc stability by blockade of new protein synthesis using cycloheximide showed that MLN8054 accelerated the turnover of approximately 70% of

(D) IMR-32 cells were preincubated with 1,000 nM MLN8054 or solvent control for 24 hr as indicated, then treated with cycloheximide (100 μg/ml), harvested at the indicated time points, and immunoblotted with the indicated antibodies. Exposures of N-Myc blots were adjusted to equalize exposure at 0 min (n = 5).
(E) Quantification of five independent N-Myc stability assays performed as described in (D). Data are plotted as mean ±SEM. Levels of N-Myc at 0 min were set to 1 for both conditions (***$p < 0.0001$; **$p < 0.02$; differences at later time points were not statistically significant).
(F) IMR-32 cells were pretreated with 1,000 nM MLN8054 or solvent control for 24 hr as indicated and subsequently labeled with ^{35}S-labeled methionine. The panel shows immunoprecipitations using N-Myc antibodies or controls after the indicated chase times.
(G) Quantitation of N-Myc stability assays. The panel shows the average (mean ±SEM) of three independent pulse-chase experiments performed as described in (F) in IMR-32 cells (**$p < 0.02$; *$p < 0.05$).
(H) IMR-32 cells were treated for 14 hr with 1,000 nM MLN8054 in the presence or absence of MG132 (5 μM) and then immunoblotted for the indicated proteins (n = 2).
See also Figure S1.

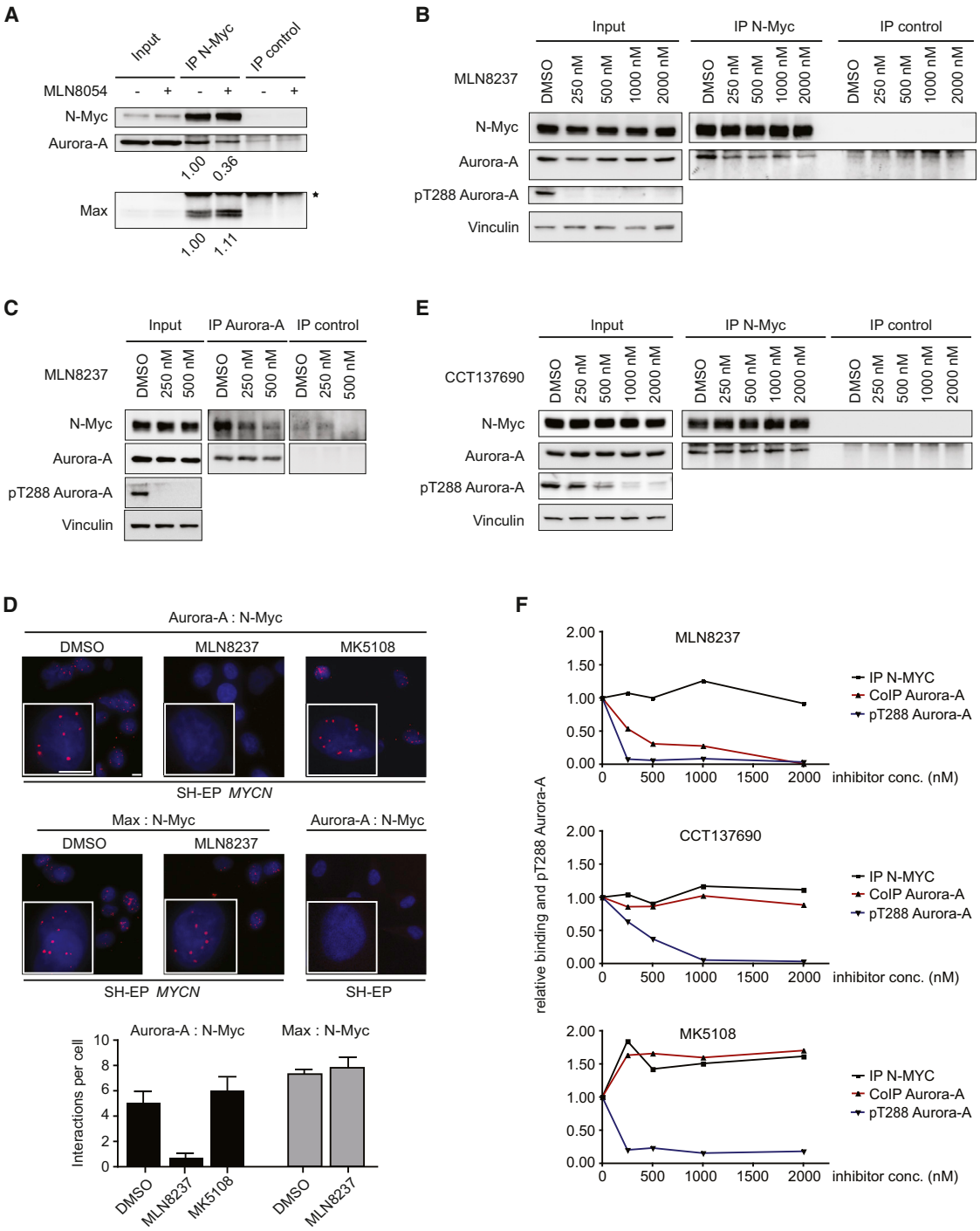

Figure 2. Structurally Related Aurora-A Inhibitors Dissociate Aurora-A/N-Myc Complexes

(A) IMR-32 cells were treated with MLN8054 (1,000 nM, 4 hr) in the presence of MG132 (5 μM). Subsequently, cell lysates were immunoprecipitated with either control or N-Myc antibodies and probed with the indicated antibodies. Input: cell lysate loading control. Relative amounts of Aurora-A and of Max recovered in N-Myc immunoprecipitates are indicated below each panel (n = 4). Asterisk indicates light chain of antibody.

(B) The experiment was performed as described in (A) in the presence of the indicated concentrations of MLN8237 (n = 2).

(C) IMR-32 cells were treated with either DMSO or the indicated concentrations of MLN8237 (4 hr) in the presence of MG132. Subsequently, cell lysates were immunoprecipitated with either control or Aurora-A antibodies. Immunoblots depict amounts of the indicated proteins (n = 4). Input: cell lysate loading control.

(D) Proximity ligation assays analyzing N-Myc/Aurora-A and N-Myc/Max complexes in SH-EP cells stably expressing N-Myc. Blue, DAPI staining of nuclei; red dots, PCR amplification products indicating complex formation of N-Myc with Aurora-A or with Max as indicated. Scale bars indicate 10 μm. Where indicated, MLN8237 (500 nM) or MK5108 (1,000 nM) was added for 4 hr (n = 3). SH-EP cells not expressing N-Myc serve as negative control. Lower panel shows mean +SD of triplicate biological replicates.

(legend continued on next page)

total N-Myc protein, whereas the remaining pool of N-Myc was more stable (Figures 1D and 1E). Similarly, pulse-chase experiments showed that about half of newly synthesized, endogenous N-Myc protein was rapidly degraded in the presence of MLN8054 in IMR-32 cells (Figures 1F and 1G). The same result was obtained using MLN8237 (Figure S1I). Furthermore, MLN8054 destabilized the ectopically expressed N-Myc protein in SH-EP cells (Figure S1J). Finally, the effect of MLN8054 was reverted by addition of the proteasome inhibitor, MG132 (Figure 1H). We concluded that MLN8054 and MLN8237 stimulate degradation of N-Myc by the proteasome. The data also suggest that MLN8054 selectively destabilizes a pool of N-Myc that is sensitive to degradation by Fbxw7 in mitosis; this hypothesis is tested below.

Destabilization of N-Myc might be either an indirect consequence of cell-cycle arrest in G2/M due to inhibition of the catalytic activity of Aurora-A or a specific effect of MLN8054 or MLN8237 on Aurora-A/N-Myc complexes. To discern between these possibilities, we compared the effect of different Aurora-A inhibitors on N-Myc levels, N-Myc/Aurora-A complexes, and cell-cycle progression. Addition of MLN8054 or MLN8237 decreased the amount of Aurora-A that coimmunoprecipitated with N-Myc when either compound was added to IMR-32 neuroblastoma cells in the presence of the proteasome inhibitor MG132 to block degradation of N-Myc (Figures 2A and 2B). Conversely, about 1% of total N-Myc was recovered in Aurora-A immunoprecipitates from IMR-32 cells, and incubation with MLN8237 in the presence of MG132 reduced this amount (Figure 2C). In contrast, MLN8054 had no effect on the amount of Max that bound to N-Myc, demonstrating that it specifically disrupts the N-Myc/Aurora-A complex (Figure 2A). Proximity ligation assays revealed that the Aurora-A/N-Myc complex is present in the nucleus and in the cytosol of virtually all interphase cells and showed that both MLN8237 and MLN8054 decreased the amount of the complex by approximately 80%, consistent with the results obtained in immunoprecipitation experiments (Figure 2D; data not shown) (Gullberg et al., 2003). MLN8054 also decreased the amount of N-Myc bound to Aurora-A when the immunopurified complex was incubated with the compound in vitro, demonstrating that MLN8054 acts directly on the complex (Figure S2A).

As expected from inhibition of the Aurora-A kinase activity, two selective Aurora-A inhibitors with dissimilar chemical structures, MK5108 and CCT137690, also induced accumulation of IMR-32 cells in the G2/M phase to the same extent as MLN8054 and MLN8237 (Figure S1F) (Seki et al., 2008). Unlike MLN8054 and MLN8237, however, neither MK5108 nor CCT137690 nor the pan-Aurora inhibitor Hesperadin disrupted the Aurora-A/N-Myc complex (Figures 2D–2F and S2B) (Faisal et al., 2011; Shimomura et al., 2010). Importantly, extensive titrations of MLN8054, MLN8237, and MK5108 in multiple cell lines showed that the ability to dissociate the Aurora-A/N-Myc complex correlated with the ability to decrease N-Myc levels (Figure S2C). We concluded that destabilization of N-Myc requires dissociation of Aurora-A/N-Myc complexes by MLN8054 or MLN8237.

Titration of MLN8054 and MLN8237 revealed that the IC_{50} values for the decrease in N-Myc levels and for dissociation of the Aurora-A/N-Myc complex are significantly higher than the concentration required for inhibition of the autophosphorylation of Aurora-A at T288 (Figures 2B, 2F, S2C, S3A, and S3B). Assuming that the accessibility of the Aurora-A/N-Myc complex is equal to that of free Aurora-A, this difference might reflect the additional energy required to disrupt the Aurora-A/N-Myc complex. Alternatively, this elevated IC_{50} value reflects an off-target effect of the drug. To distinguish between these possibilities, we expressed doxycycline-inducible alleles of either wild-type Aurora-A or Aurora-AT217D, a mutant allele that has a reduced affinity toward MLN8054, in *MYCN*-amplified SMS-KCN neuroblastoma cells (Sloane et al., 2010). The addition of MLN8054 suppressed colony formation of control cells and of cells expressing wild-type Aurora-A (Figure 3A). In contrast, cells that expressed Aurora-AT217D were capable of colony formation in the presence of MLN8054, and Aurora-A kinase remained active under these conditions (Figures 3A and 3B). Importantly, cells expressing Aurora-AT217D maintained elevated N-Myc levels in the presence of MLN8054, in contrast to control cells or cells expressing wild-type Aurora-A (Figure 3B). Furthermore, immunoprecipitation assays revealed that the N-Myc/Aurora-AT217D complex remained stable in the presence of MLN8054 (Figure 3C). As an additional control to demonstrate that the ability to inhibit N-Myc expression is an on-target activity of MLN8054, we used a small series of structurally related compounds with well-characterized affinities toward Aurora-A. The ability of these compounds to affect N-Myc expression paralleled their inhibition of Aurora-A, further supporting the notion that MLN8054 and structurally related compounds regulate N-Myc levels via dissociation of an Aurora-A/N-Myc complex (Figure 3D).

A key ubiquitin ligase that mediates ubiquitination of N-Myc is Fbxw7 (Welcker et al., 2004; Yada et al., 2004). Fbxw7 recognizes N-Myc after sequential phosphorylation at S62 by cyclin B/CDK1, which primes N-Myc for phosphorylation at T58 by GSK3β (Sjostrom et al., 2005; Yeh et al., 2004). Consequently, Fbxw7 does not recognize a mutant allele of N-Myc, which carries alanine substitutions at both residues (N-MycT58AS62A = $N\text{-}Myc_{mut}$) (Sjostrom et al., 2005). This mutant is neither bound nor stabilized by Aurora-A, suggesting that Aurora-A specifically antagonizes degradation by Fbxw7 (Otto et al., 2009). Consistent with these observations, MLN8054 decreased levels of ectopically expressed N-Myc, but not $N\text{-}Myc_{mut}$, in SH-EP neuroblastoma cells that do not express endogenous N-Myc (Figure 4A). Depletion of Fbxw7 in IMR-32 cells enhanced steady-state levels of endogenous N-Myc and abolished the MLN8054-induced decrease in N-Myc levels, whereas depletion of HectH9/Huwe1, another ubiquitin ligase that is involved in the

(E) IMR-32 cells were treated with the indicated concentrations of CCT137690 (4 hr) in the presence of MG132. N-Myc/Aurora-A complexes were analyzed as described in (B).
(F) Quantitation of Aurora-A/N-Myc complexes in response to treatment with MLN8237, CCT137690, and MK5108. Data are shown for one experiment for each inhibitor performed as described above.
See also Figure S2.

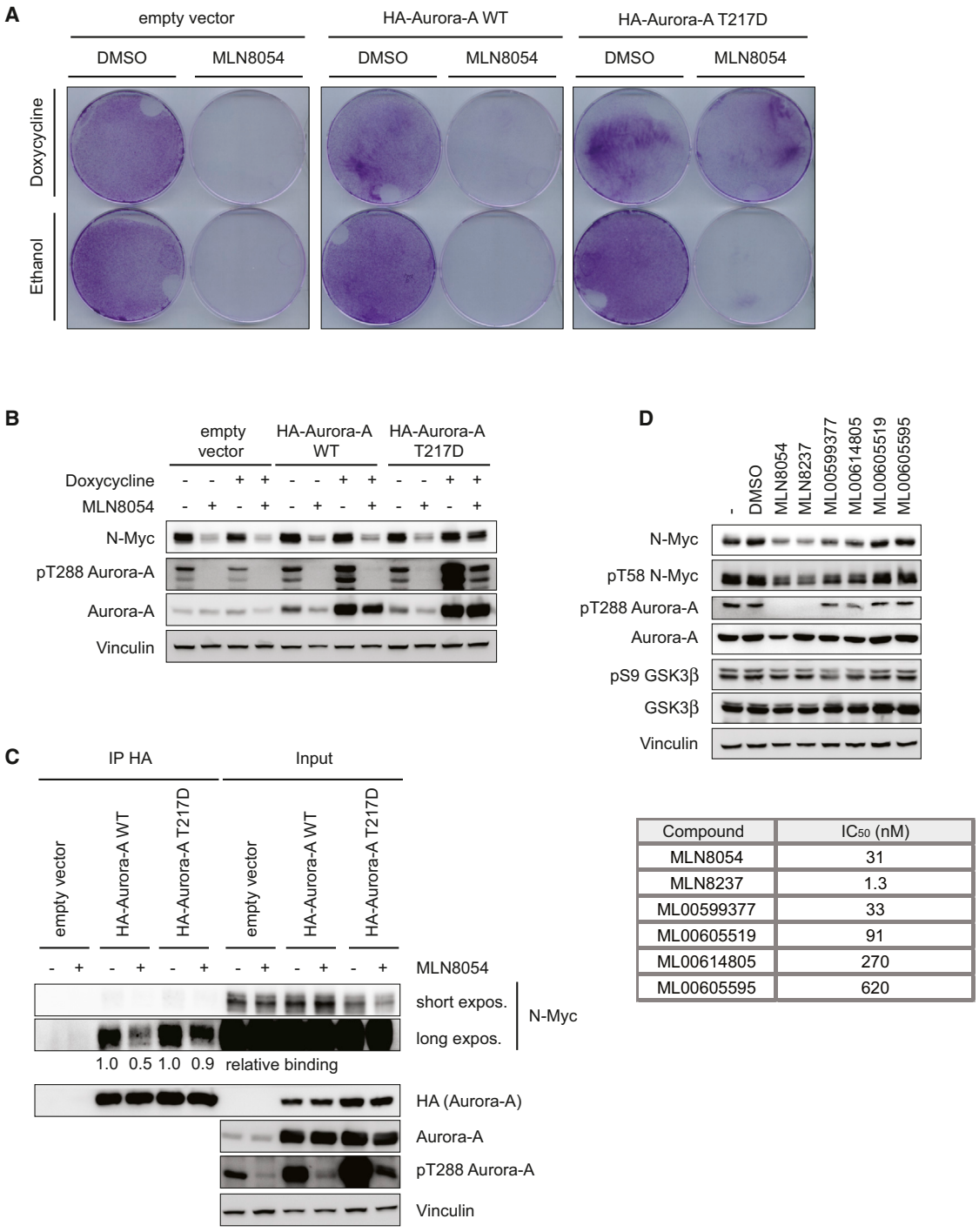

Compound	IC_{50} (nM)
MLN8054	31
MLN8237	1.3
ML00599377	33
ML00605519	91
ML00614805	270
ML00605595	620

Figure 3. Effects of Aurora-A Inhibitors on N-Myc in Cells Expressing Wild-Type Aurora-A and Drug-Resistant Aurora-AT217D

(A) *MYCN*-amplified SMS-KCN cells were stably transduced with expression plasmids encoding a tetracycline-dependent transactivator. They were subsequently stably transduced with control vector or vector expressing hemagglutinin (HA)-tagged wild-type Aurora-A or Aurora-AT217D. Pools of cells were subsequently treated with MLN8054 (500 nM) and doxycycline (1 μg/ml) as indicated. The panels show colony assays stained with crystal violet 4 days later (n = 3).

(B) Immunoblot analysis of the SMS-KCN cells described in (A) depicting expression of the indicated proteins; MLN8054 was added for 48 hr (500 nM) (n = 3).

(C) The SMS-KCN cells described in (A) were treated with MLN8054 (2,000 nM; 4 hr) in the presence of MG132 (5 μM) and doxycycline (1 μg/ml; 12 hr) as indicated. Cell lysates were prepared and immunoprecipitated with HA antibodies. The panels show immunoblots probed with the indicated antibodies. Levels of N-Myc recovered in HA immunoprecipitates (relative to DMSO-treated cells) are indicated below each lane (n = 2).

(D) IMR-32 cells were incubated with the indicated series of MLN8054 derivatives (1,000 nM; 24 hr). The upper panels show immunoblots of cell lysates probed with the indicated antibodies (n = 3). IC_{50} data of these compounds from in vitro assays of Aurora-A kinase are shown at the bottom.

See also Figure S3.

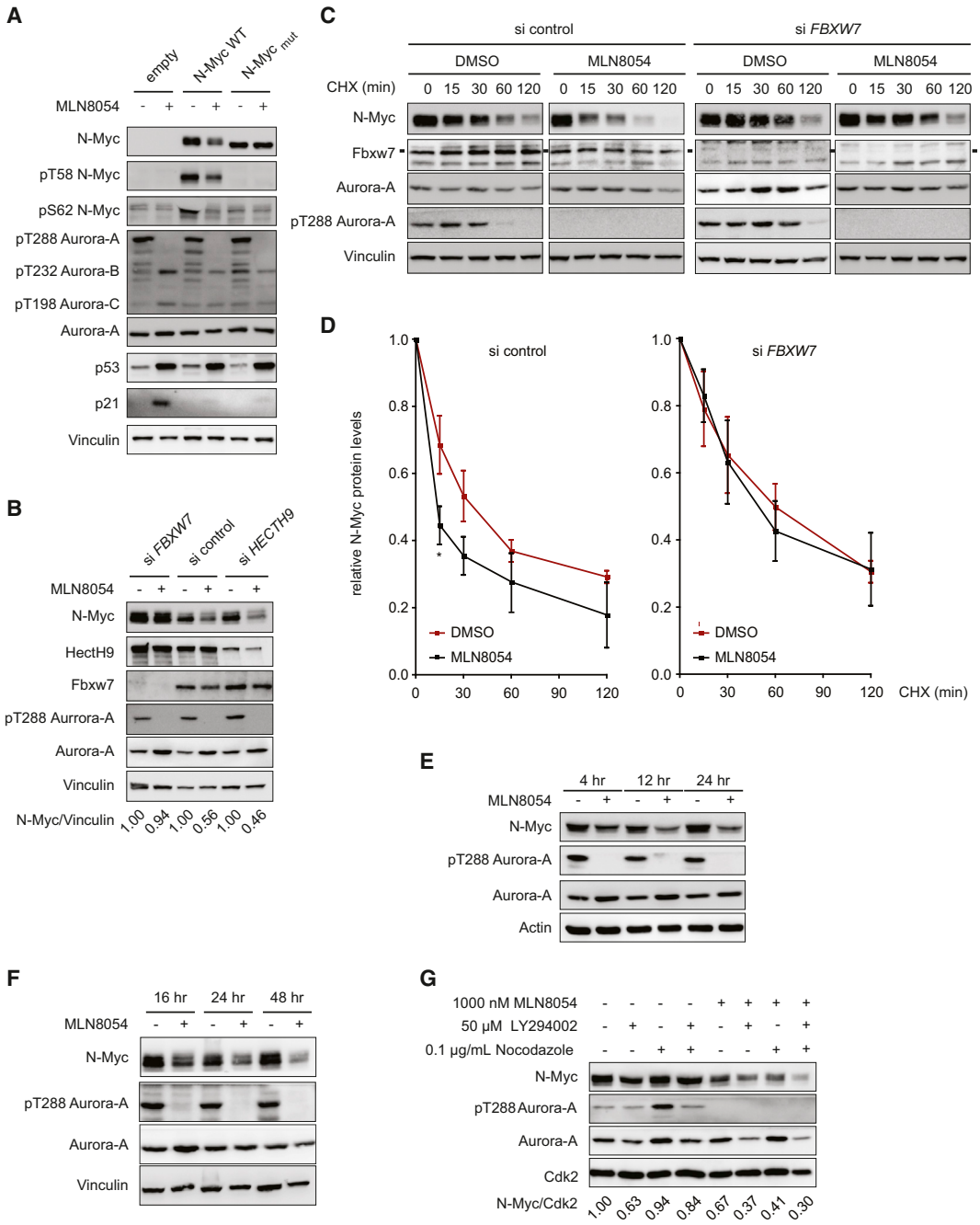

Figure 4. Role of Fbxw7 in MLN8054-Induced Degradation of N-Myc

(A) SH-EP cells were stably transduced with retroviruses expressing either N-Myc (WT) or N-MycT58AS62A (mut) then incubated with MLN8054 (1,000 nM; 48 hr) or solvent control as shown. The panels show immunoblots of cell lysates probed with the indicated antibodies (n = 3).

(B) Immunoblots of IMR-32 cells that were transfected with indicated siRNAs. Cells were incubated with MLN8054 or solvent control for 24 hr and analyzed as in panel A (n = 3). Ratios of N-Myc to vinculin are indicated below the panel.

(C) IMR-32 were transfected with siRNA targeting *FBXW7* or control siRNA. Then 24 hr before harvesting, cells were treated with MLN8054 (1,000 nM) or DMSO as control. CHX was added for the indicated times. Exposures of N-Myc blots were adjusted to equalize exposure at 0 min (n = 3).

(D) Quantification of three independent stability experiments performed as described for (C). Levels of N-Myc at 0 min were set to 1 for all conditions. Values are shown as mean ±SEM (*p < 0.02 relative to siFbxw7-treated cells).

(E) SH-EP cells engineered to stably express wild-type N-Myc were incubated with MLN8054 (1,000 nM) for the times shown. Immunoblots depict expression of the indicated proteins (n = 2).

(F) IMR-32 were incubated with MLN8054 (1,000 nM) for the indicated times before lysates were prepared and blotted as before.

(G) IMR-5 neuroblastoma cells were incubated with the indicated drugs for 18 hr. The panels show immunoblots of cell lysates probed with the indicated antibodies. Amounts of N-Myc relative to Cdk2 are indicated below each lane (n = 2).

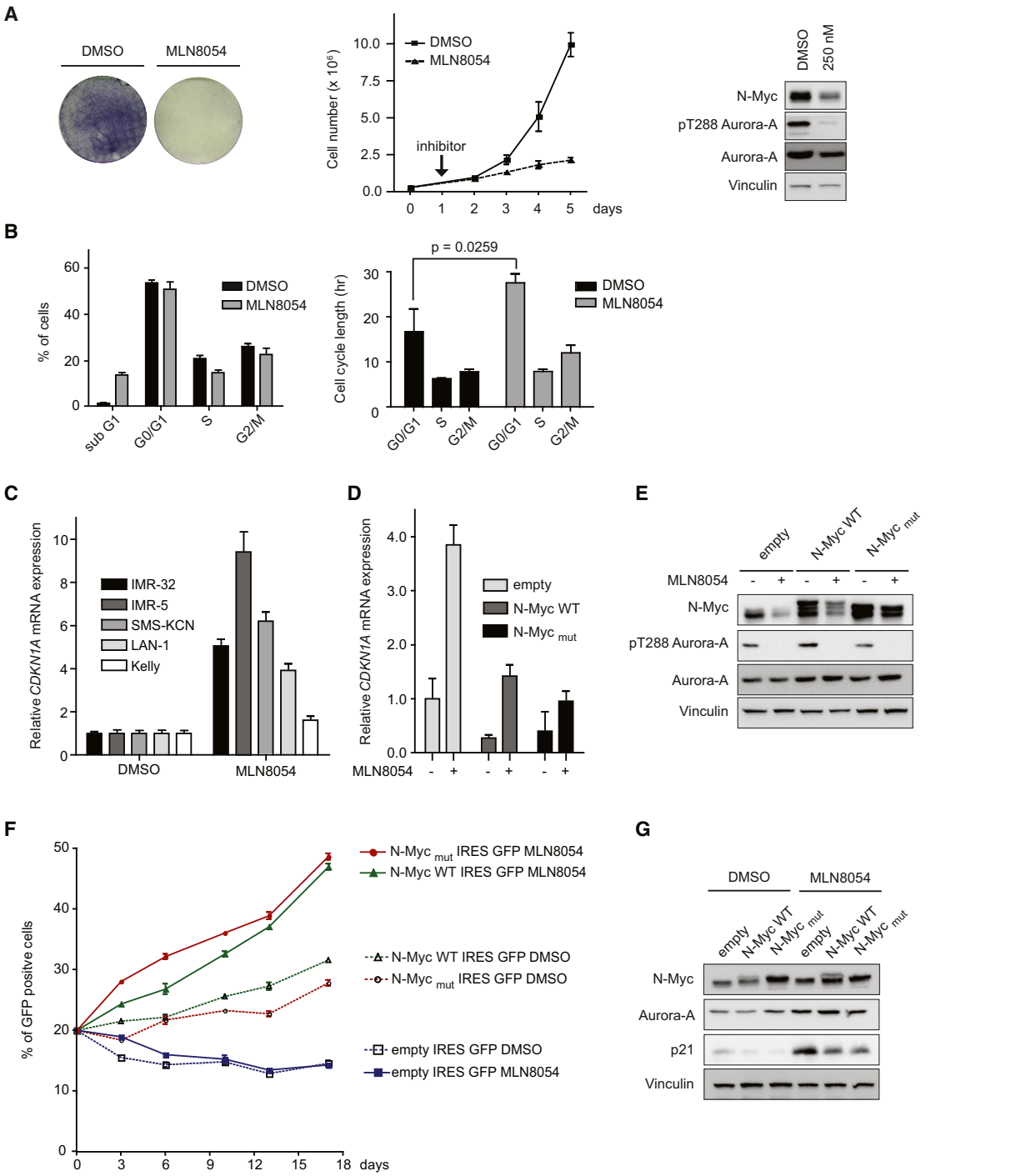

Figure 5. Role of N-Myc in Cellular Responses of *MYCN*-Amplified Neuroblastoma Cells to MLN8054

(A) The panel on the left shows crystal violet-stained culture dishes of SMS-KCN cells grown in the presence of MLN8054 (250 nM) or solvent control for 4 days. The graph in the middle documents proliferation of SMS-KCN cells under the same conditions. Error bars indicate SD of triplicate biological replicates. Immunoblots on the right depict levels of the indicated proteins 48 hr after addition of MLN8054.

(B) FACS analysis showing cell cycle phases of SMS-KCN cells in response to MLN8054 (250 nM; 48 hr) (left). The data were combined with the growth curve shown in (A) to calculate the length of each cell-cycle phase (right). Error bars indicate SD of triplicate biological replicates.

(C) The graph shows levels of *CDKN1A* mRNA relative to β2-microglobulin and *RPS14* as control determined by quantitative RT-PCR. The indicated cell lines were incubated with MLN8054 (1,000 nM) or DMSO for 48 hr before RNA was prepared. Error bars indicate SD of triplicate technical replicates from one of two experiments with identical results.

(D) LAN-1 cells were stably transduced with lentiviruses expressing either wild-type N-Myc or N-Myc$_{mut}$ and the experiment performed as described in (C). Error bars indicate SD of triplicate technical replicates.

(legend continued on next page)

ubiquitin-mediated degradation of N-Myc, had no significant effect (Figure 4B). Importantly, depletion of Fbxw7 stabilized N-Myc and reverted the enhanced turnover of N-Myc in the presence of MLN8054 (Figures 4C and 4D). Note that because the depletion of HectH9/Huwe1 is not complete, we cannot rule out a contribution of residual HectH9/Huwe1 to N-Myc turnover in response to MLN80454.

The addition of MLN8054 for 24 hr destabilized about 50%–70% of total N-Myc protein, suggesting that a specific pool of N-Myc is sensitive to MLN8054; this corresponds to the fraction of cells that are in G2/M upon inhibitor treatment. Furthermore, overall levels of N-Myc decreased progressively over 24–48 hr in response to MLN8054, suggesting that MLN8054 might destabilize N-Myc when cells have progressed to G2 and M phase (Figures 4E and 4F). Degradation of N-Myc by Fbxw7 is initiated by the mitotic kinase, cyclin B/CDK1 (Sjostrom et al., 2005). As a result, depletion of Aurora-A strongly affects N-Myc levels in cells synchronized in mitosis by the addition of nocodazole; degradation is further enhanced by inhibition of PI3-kinase, which activates GSK3β to phosphorylate T58 of N-Myc (Otto et al., 2009). Similarly, addition of MLN8054 enhanced N-Myc turnover in response to PI3-kinase inhibition by LY294002 in nocodazole-treated cells (Figure 4G). The same result was obtained using the dual PI3-kinase/mTOR inhibitor BEZ235 (not shown). The data strongly suggest that Aurora-A protects N-Myc from Fbxw7-mediated degradation during mitosis and that the slow kinetics of decrease is due to the requirement for mitotic phosphorylation of N-Myc.

Incubation with MLN8054 suppressed colony formation and inhibited proliferation of all *MYCN*-amplified neuroblastoma cell lines that we tested (Figures 5A and S4A). IC_{50} values for suppression of proliferation of *MYCN*-amplified neuroblastoma lines range between 250 and 700 nM, consistent with the possibility that downregulation of N-Myc contributes to growth inhibition (Shang et al., 2009). FACSscan experiments showed that the predominant response of *MYCN*-amplified SMS-KCN cells to treatment with MLN8054 was a delay in progression through both the G1 and the G2 phase of the cell cycle, similar to the response elicited by small hairpin RNA-mediated depletion of Aurora-A (Figure 5B) (Otto et al., 2009). Prolonged incubation with MLN8054 also induced varying degrees of apoptosis in *MYCN*-amplified neuroblastoma cell lines (Figure 5B; data not shown). While the delay in progression through G2 is likely to reflect catalytic functions of Aurora-A in mitotic entry (see above), we speculated that the delay in progression through the G1 phase may depend on degradation of N-Myc. Consistent with previous observations that N-Myc represses expression of the cell-cycle inhibitor *CDKN1A* (encoding $p21^{Cip1}$) (Herold et al., 2002), incubation with MLN8054 induced a significant increase in expression of *CDKN1A* in four out of five *MYCN*-amplified cell lines tested (Figure 5C). Induction of *CDKN1A* in response to MLN8054 was independent of p53 status, since it also occurred in LAN-1 cells that do not express detectable p53 and, to a lesser degree, in Kelly cells (Figure 5C) and since it was not blocked by expression of a dominant-negative allele of p53 (Figures S4B and S4C). Ectopic expression of N-Myc or $N\text{-}Myc_{mut}$ in *MYCN*-amplified cells attenuated induction of *CDKN1A*, arguing that elimination of *MYCN* is required for induction of *CDKN1A* expression (Figure 5D). Note that the ectopically expressed N-Myc protein was not completely degraded in the presence of MLN8054 in these experiments (Figure 5E). Identical results were obtained in SHEP cells ectopically expressing or N-Myc or $N\text{-}Myc_{mut}$ (Figure 4A). Importantly, ectopic expression of N-Myc and $N\text{-}Myc_{mut}$ provided a moderate proliferative advantage to *MYCN*-amplified cells in the absence of MLN8054 but a much stronger advantage in the presence of MLN8054 (SMS-KCN cells: Figure 5F; IMR-5 cells: data not shown). This correlated with their ability to suppress MLN8054-induced expression of $p21^{Cip1}$ (Figure 5G). We concluded that elimination of N-Myc is required for the complete arrest of cell proliferation and for the induction of $p21^{Cip1}$ expression by MLN8054 in cultured *MYCN*-amplified neuroblastoma cells.

Murine Aurora-A binds to the human N-Myc protein (Figure S5A), allowing us to use the TH-*MYCN* mouse model of aggressive neuroblastoma, in which high-level expression of *MYCN* is driven in neural crest by a tyrosine hydroxylase (TH) promoter, to evaluate the therapeutic efficacy of MLN8054 and MLN8237 in an in vivo setting (Weiss et al., 1997). Mice with large established tumors were initially treated with daily oral administration of 40 mg/kg MLN8054. After 3 days of treatment, immunoblots revealed a large decrease in N-Myc protein in four out of six tumors and a modest decrease in two out of six tumors in comparison to vehicle-treated tumors (Figure 6A). Treatment with 30 mg/kg MLN8237 induced more rapid decreases in tumor volume ($p = 0.022$; Figure S5B), and downregulation of N-Myc was observed in eight out of eight tumors after 24 hr ($p = 0.0023$; Figure S5C). Downregulation of N-Myc occurred post-translationally, since levels of human and mouse *MYCN* mRNA were unaffected by MLN8054 or MLN8237 (Figure S5D). To test whether MLN8054 affects the amount of N-Myc bound to its target sites in vivo, we performed chromatin immunoprecipitation (ChIP) experiments from three vehicle- and three MLN8054-treated mice. These experiments revealed that N-Myc specifically bound to the E-box of the *Apex* promoter, a well-characterized target gene of N-Myc, and that treatment with MLN8054 strongly reduced binding to this site (Figure 6B). Identical results were obtained for the Myc-binding sites localized in the *Ncl1* and *Slc25a19* genes (not shown). To

(E) Immunoblots documenting expression of N-Myc or $N\text{-}Myc_{mut}$ in LAN-1 cells exposed to MLN8054 (1,000 nM; 48 hr) or solvent control. Note that the ectopically expressed N-Myc is not completely degraded in response to MLN8054.
(F) SMS-KCN cells were infected with either control viruses (empty) or retroviruses expressing N-Myc or $N\text{-}Myc_{mut}$ together with a GFP marker. Cells were mixed with uninfected cells such that 20% of cells expressed GFP at the start of the experiment. The graph shows the percentage of GFP-positive cells during culture in the absence or presence of MLN8054 (100 nM). Error bars represent SD of triplicate biological samples. From the data, the following doubling times can be estimated: control cells: DMSO: 26 hr; MLN8054: 36 hr; N-Myc- and $N\text{-}Myc_{mut}$-expressing cells: DMSO: 25 hr; MLN8054: 32 hr (n = 2).
(G) Immunoblots documenting expression of the indicated proteins at the end of the experiment shown in (F). Note that cells growing in the presence of MLN8054 have selected for elevated levels of N-Myc.
See also Figure S4.

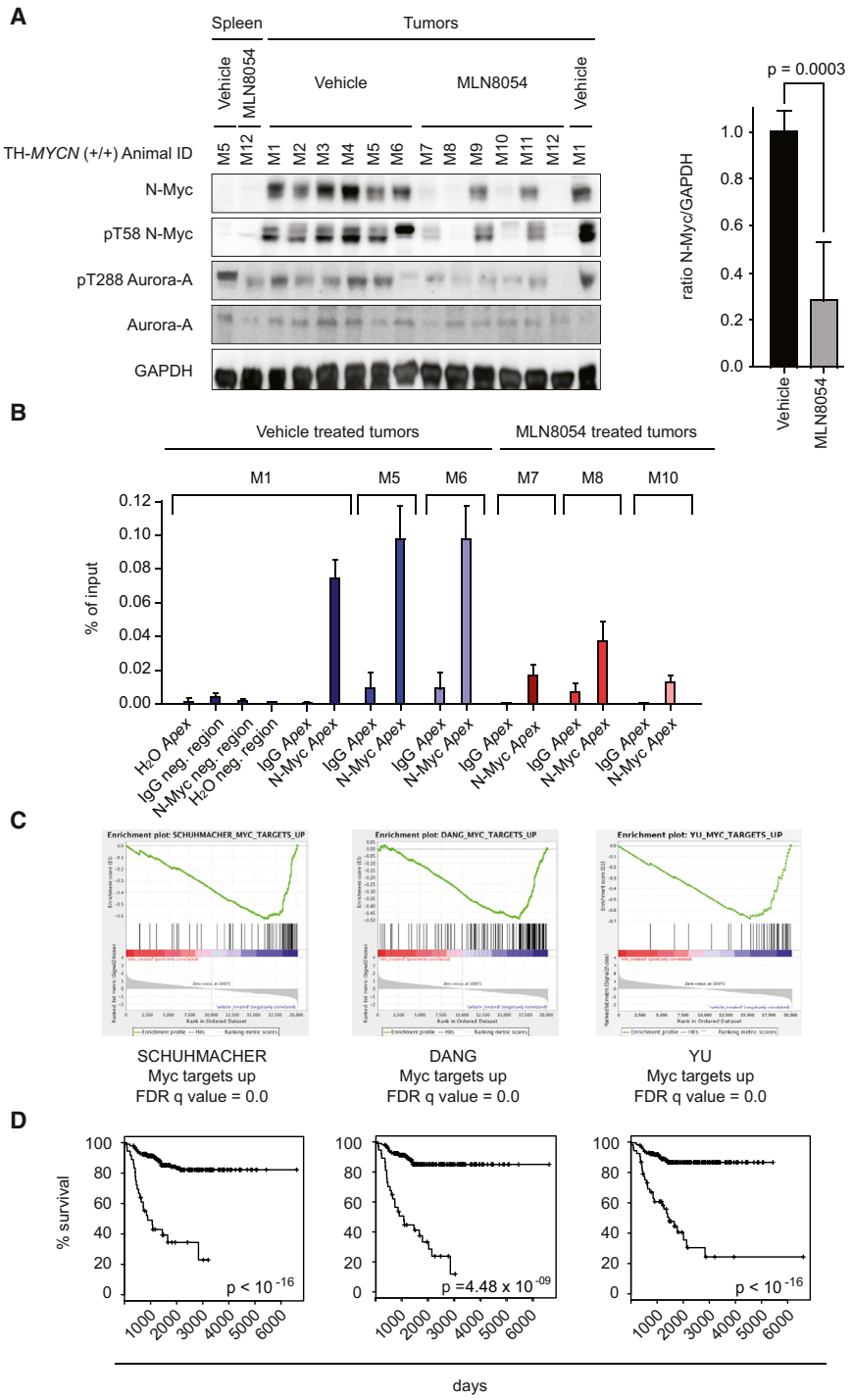

Figure 6. Effects of MLN8054 on N-Myc Function in TH-*MYCN* Neuroblastoma Mice

(A) Tumor-bearing TH-*MYCN* mice were treated for 3 days with 40 mg/kg MLN8054 or vehicle. The panels on the left show immunoblots of lysates of neuroblastomas probed with the indicated antibodies. Spleen tissue is included as negative control for N-Myc antibody. The panel on the right shows a quantification of the immunoblot (data are plotted as mean +SEM).

(B) Results of ChIP assays using N-Myc or control antibodies at a genomic region surrounding the E box of the *Apex* gene or a negative control region as indicated. Error bars indicate SD of triplicate technical replicates.

(C) RNA was isolated from four MLN8054-treated and from four vehicle-treated neuroblastomas and subjected to microarray analysis. The panels show expression of well-characterized gene sets of *MYC*-regulated genes and their response to MLN8054 treatment.

(D) The graphs show Kaplan-Meier diagrams of human patients stratified by the expression levels of the gene sets shown in (C). Graphs and p values are shown for overall survival.

See also Figure S5.

determine how the observed decreases in N-Myc affect the transcriptional functions of N-Myc, we used microarrays to compare gene expression profiles of four MLN8054-treated tumors against four vehicle-treated tumors. Gene set enrichment analysis (GSEA) showed strong modulation of expression of multiple Myc target gene sets in response to MLN8054, demonstrating that MLN8054 interferes with N-Myc-dependent transcription in vivo (Figure 6C) (Subramanian et al., 2005). The prognostic relevance of gene sets regulated by MLN8054 was investigated in a cohort of 476 primary neuroblastomas representing the entire spectrum of the disease (Oberthuer et al., 2010). Prognostic classifiers based on MLN8054-regulated gene sets were generated in a training set comprising approximately half of the total cohort, and their classification performance was evaluated in the remaining test set. Importantly, we observed that gene sets regulated by MLN8054 in the mouse model were strongly associated with both overall (Figure 6D) and event-free survival (Figure S5E) of neuroblastoma patients. We concluded that treatment with MLN8054 interferes with critical oncogenic functions of N-Myc in vivo.

GSEA analysis also provided evidence that MLN8054 reduced expression of genes that are characteristic of pluripotent stem cells, suggesting that MLN8054 limits the self-renewal capacity of neuroblastoma cells (Figure S5F) (Wong et al., 2008). In support of this contention, treatment with MLN8054 abolished the ability of IMR-5 cells to grow as neurospheres in culture (Figure S5G). MLN8054 also downregulated N-Myc, abolished clonogenic growth, and induced expression of neurofilament protein L mRNA (*NEFL*), a marker of differentiation, in a primary neurosphere culture derived from a patient with bone marrow metastasis, supporting the notion that the MLN8054 results extend to human disease (Figures S5H and S5I).

Analysis of tumor volume response by MRI revealed complete response rates around 50% for both compounds (Figures 7A, 7B, S6A, and S6B; four out of nine complete responses with MLN8054 and five out of eight complete responses with MLN8237). Histological analysis of tumors recovered from mice after 1 day (MLN8237) or 3 days (MLN8054) of treatment revealed highly significant increases in mitotic activity, with neuronal differentiation consistent with partial maturation of tumors, and inflammatory infiltrates (Figures 7C and S6C). There were also prominent sheets of foamy histiocytes, indicative of inflammation. Immunohistological analysis showed that both drugs increased the percentage of cells staining positively for phosphoH3, indicative of an accumulation in G2 and mitosis (Figures 7D, S6C; quantification of staining is in Figure S6D for MLN8054 and S6E for MLN8237). In addition, there was a decrease in N-Myc staining intensity, supporting the immunoblot data. Consistent with the reduction of clonogenic growth observed in vitro, treatment with MLN8054 increased the number of cells staining positively for the senescence marker $H3K9^{me}$ and decreased expression of Bmi1, which is critical for the self-renewal of neuronal progenitor cells (Bruggeman et al., 2005). Neither MLN8054 nor MLN8237 induced a significant increase in apoptotic cells. Finally, treatment with MLN8054 induced infiltration of immune cells, including macrophages (stained with Mac2) and T-lymphocytes (Figure 7D; data not shown).

Exposure of tumor-bearing mice to 40 mg/kg MLN8054 resulted in rapid tumor regression. However, this high dose was not tolerated well in long-term experiments, which complicated the interpretation of survival studies (not shown). A lower split dose of 15 mg/kg twice daily was well tolerated, significantly extended survival ($p = 0.0016$), and decreased N-Myc levels in vivo (Figures 7E and S6F). Treatment with MLN8237 was well tolerated and resulted in a more pronounced extension of survival (Figure 7F; $p = 0.0004$). In similar trials, neither MK5108 nor CCT137690 had significant effects on survival, tumor growth, or N-Myc levels (data not shown). However, mass spectrometry and immunoblots of Aurora-A^{T288P} revealed that effective intratumoral levels of either compound were variable even at high oral doses, precluding a definitive assessment of their efficacy. Taken together, our data show that both MLN8054 and MNL8237 effectively destabilize the N-Myc protein, cause a blockade of N-Myc function, and achieve significant therapeutic benefit in this in vivo model of neuroblastoma.

DISCUSSION

The N-Myc protein differs from the founding member of the family, c-Myc, in that degradation of N-Myc is initiated via phosphorylation by cyclin B/CDK1 and therefore tightly linked to mitosis (Sjostrom et al., 2005). The mitotic degradation of N-Myc is thought to allow cell-cycle exit and differentiation of neuroblasts. In human neuroblastoma cells, Aurora-A forms a complex with the N-Myc protein that stabilizes N-Myc in mitosis, thereby maintaining neuroblastoma cells in a proliferative state (Otto et al., 2009). We show here that MLN8237 and MLN8054 disrupt the Aurora-A/N-Myc complex. Phosphorylation of N-Myc by cyclin B/CDK1 initiates ubiquitination of N-Myc by Fbxw7 (Welcker et al., 2004; Yada et al., 2004). Consistently, we found that Fbxw7 is required for degradation of N-Myc in response to disruption of the Aurora-A/N-Myc complex. The exact mechanism by which complex formation of N-Myc with Aurora-A prevents degradation of N-Myc is currently unknown. Notably, approximately 1% of N-Myc was recovered in Aurora-A immunoprecipitates, arguing that Aurora-A does not act by sterically blocking the access of Fbxw7 to N-Myc. Rather, we suggest that Aurora-A recruits a stabilizing activity; possible candidates are a S62 phosphatase such as PP2A or a deubiquitinating enzyme such as Usp28 (Horn et al., 2007; Popov et al., 2007) (Figure 8).

In response to MLN8054 or MLN8273, N-Myc levels decreased progressively over a 24–48 hr time period, which cannot be explained by the short half-life of N-Myc. Proximity-ligation assays showed that the Aurora-A/N-Myc complex is detectable in virtually all cells. We propose, therefore, that the slow kinetics of N-Myc degradation reflects the need for cyclin B/CDK1 to phosphorylate N-Myc in mitosis. Since inhibition of the catalytic activity of Aurora-A delays entry into mitosis (Seki et al., 2008), we suggest that purely allosteric inhibitors of Aurora-A, which disrupt the Aurora-A/N-Myc complex but do not inhibit the catalytic activity of Aurora-A, may have a more rapid impact on N-Myc levels.

Treatment with MLN8054 broadly inhibits N-Myc dependent transcription in vivo. Genes that are downregulated in response to MLN8054 are prognostically significant in human neuroblastoma. They include genes that mediate oncogenic functions of Myc and that in turn have been proposed to be therapeutic targets for Myc-dependent tumors, such as ODC1 and CDK4 (Miliani de Marval et al., 2004; Nilsson et al., 2005). In addition, treatment of neuroblastomas with MLN8054 or MLN8237 induces senescence and differentiation as well as infiltration of immune cells, phenotypes that are thought to mediate tumor regression in response to inhibition of Myc in regulatable mouse tumor models (Rakhra et al., 2010; Sodir et al., 2011). Consistent with induction of senescence, MLN8054 diminishes expression of Bmi1, which is a critical regulator of stem cell functions, and represses a stem cell-specific gene expression program. We suggest that these effects contribute to the ability of MLN8054 and MLN8237 to prolong survival in the N-Myc-dependent mouse model of neuroblastoma. This remains to be formally proven, since MK5103 and CCT137690, which did not disrupt the Aurora-A/N-Myc complex in culture and did not affect survival in the TH-*MYCN* model, did not consistently accumulate to high enough concentrations in the tumor tissue to allow definitive conclusions about their therapeutic efficacy. Similarly, it remains possible that the decrease in N-Myc levels observed in vivo occurs via a mechanism that is different from Fbxw7-mediated degradation.

MLN8237 is currently in phase 2 clinical evaluations for childhood neuroblastoma (NCT01154816). The plasma concentration of the drug in these trials is around 2 μM, which is sufficient to disrupt the Aurora-A/N-Myc complex (Matulonis et al., 2012). The identification of N-Myc as a critical target of this class of Aurora-A inhibitors suggests rational strategies for further therapy development. For example, structural considerations suggest that it is possible to optimize inhibitors to more strongly distort the Aurora-A structure and thereby more effectively disrupt the Aurora-A/N-Myc complex. As described above,

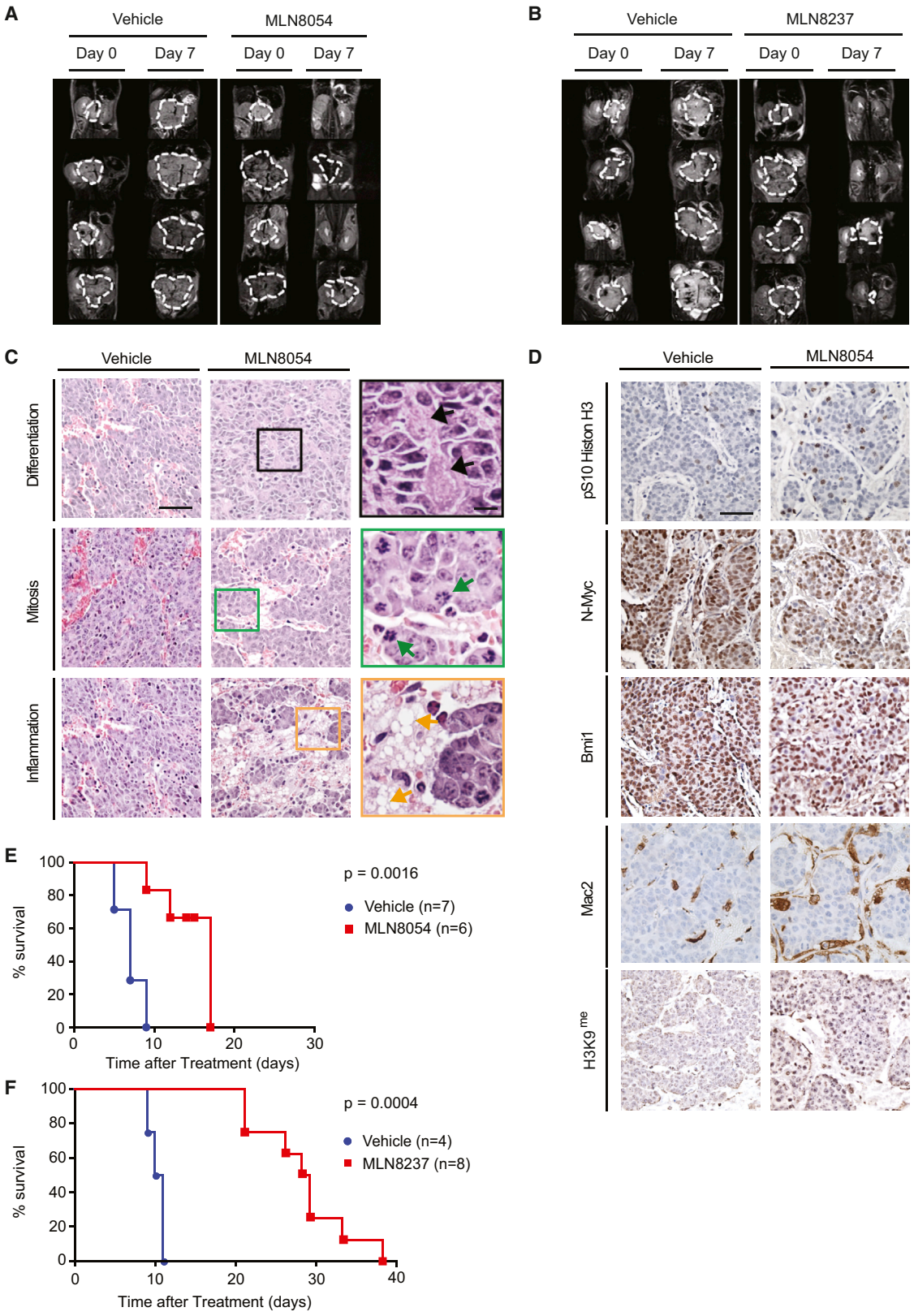

(legend on next page)

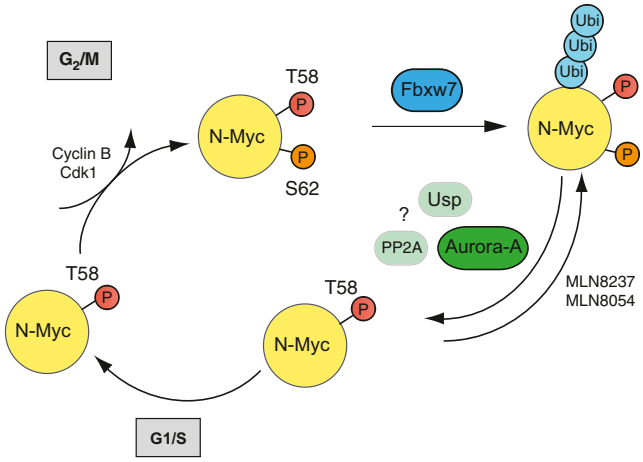

Figure 8. Model to Explain Our Findings

In normal neuroblasts, degradation of N-Myc is initiated by phosphorylation at S62 of N-Myc by cyclin B/CDK1; this primes N-Myc for phosphorylation by GSK3 at T58. The pool of doubly phosphorylated N-Myc in cells in G2/M is recognized by Fbxw7. The association of N-Myc with Aurora-A in neuroblastoma cells blocks degradation by Fbxw7 and allows N-Myc to persist into the subsequent cell cycle. MLN8237 and MLN8054 disrupt the association, thereby restoring a more physiological pattern of N-Myc degradation.

allosteric drugs can be envisaged that disrupt the Aurora-A/N-Myc complex while retaining the ability of Aurora-A to promote entry into mitosis, potentially leading to more rapid phosphorylation and degradation of N-Myc. Furthermore, degradation of N-Myc in response to MLN8054 is enhanced by inhibition of PI3-kinase, which promotes phosphorylation of N-Myc at T58 and has therapeutic efficacy in preclinical models of neuroblastoma (Chanthery et al., 2012). Similarly, small molecules targeting Brd4 allow inhibition of transcription from the *MYCN* promoter, so combinations with either drug may further decrease N-Myc protein levels below critical thresholds (Delmore et al., 2011). Our findings therefore also offer strategies to develop future combination therapies for *MYCN*-amplified neuroblastoma and potentially other N-Myc-dependent tumors.

EXPERIMENTAL PROCEDURES

Tissue Culture

Neuroblastoma cell lines were cultured in RPMI 1640 supplemented with 10% heat-inactivated fetal bovine serum. The primary neuroblastoma sphere culture was established from a highly infiltrated bone marrow aspirate of a neuroblastoma patient. Informed consent was obtained from the patient according to a research proposal approved by the institutional review board of the Medical Faculty of the University of Heidelberg. Cells were seeded in neurosphere medium (Neurobasal A, Gibco Invitrogen) supplemented with B27 serum substitute (Gibco Invitrogen), 20 ng/ml bFGF (Promokine), 20 ng/ml bFGF (Promokine), and 2 μg/ml heparin (Sigma-Aldrich) and were cultured at 37°C, 5% CO_2. For colony assays, cells were fixed with 70% ethanol and stained with crystal violet. FACS analysis was performed using propidium iodide staining of ethanol-fixed cells via a FACSCantoII(BD) flow cytometer.

In Vivo Experiments

All experimental protocols were monitored and approved by The Institute of Cancer Research Animal Welfare and Ethical Review Body, in compliance with guidelines specified by the UK Home Office Animals (Scientific Procedures) Act 1986 and the United Kingdom National Cancer Research Institute guidelines for the welfare of animals in cancer research (Workman et al., 2010). Transgenic TH-*MYCN* mice were genotyped to detect the presence of human *MYCN* transgene (Weiss et al., 1997). After weaning, animals were palpated for intra-abdominal tumors twice weekly. Mice with palpable tumors (40–80 days old) were treated with the indicated doses of MLN8054, MLN8237, or vehicle. For the MLN8054 and MLN8237 experiments shown in Figures 7E and 7F, mice were treated with indicated dose twice a day for 5 days, and then treatment was stopped for 2 days before the schedule resumed, for 2 weeks. Drugs were administered via oral gavage. Mice were allowed access to food and water ad libitum.

In Vivo Imaging and Histopathology

MRI was performed on a 7T horizontal bore microimaging system (Bruker Instruments) using a 3 cm birdcage coil. Anatomical T_2-weighted coronal images were acquired from 20 contiguous 1-mm-thick slices through the mouse abdomen, from which tumor volumes were determined using segmentation from regions of interest drawn on each tumor-containing slice. At the end of trials, tumors were dissected, divided into six approximately equal pieces, and fixed with 4% paraformaldehyde or snap frozen in liquid nitrogen. Tissue sections were stained with hematoxylin and eosin or specific antibodies. Immunohistochemistry was performed using standard methods by Histopathox Ltd. Briefly, 5 μm sections were stained with antibodies, including heat-induced epitope retrieval using citrate buffer (pH 6) or EDTA buffer, and scored by a consultant histopathologist.

Immunological Methods

Tumor or spleen tissue were homogenized using T-PER buffer (Thermo Scientific) containing 1× complete proteinase inhibitor tablet (Roche) per 10 ml buffer and a cocktail of phosphatase inhibitors (Santa Cruz). Protein concentration was measured by bicinchoninic acid assay. Protein (30 μg) was denatured in lithium dodecyl sulfate sample buffer (Invitrogen), separated on precast 4%–12% Bis-Tris gels (Invitrogen), and transferred to nitrocellulose membranes. Immunoblots were recorded electronically on a Fujifilm LAS-4000 scanner. To measure N-Myc stability, IMR-32 and SH-EP cells were pulsed for 30 min with ^{35}S-labeled methionine and chased for 0, 15, 30, or 60 min; alternatively, new protein synthesis was blocked by addition of 100 μg/ml cycloheximide. Cells were lysed with NP40 buffer, adjusted to equal incorporation, and N-Myc was immunoprecipitated using DYNAbeads. Immunoprecipitations lacking a primary antibody or with control antibodies were used as controls for specificity. ChIP experiments were performed as described elsewhere (Bouchard et al., 2001). Antibodies are listed in Supplemental Experimental Procedures.

Figure 7. In Vivo Trials of MLN8054 and MLN8237 in TH-*MYCN* Neuroblastoma Mice

(A and B) Representative day 0 and 7 MRI sections of mice treated with vehicle or 40 mg/kg MLN8054 (A) or 30 mg/kg MLN8237 (B). Dashed white lines indicate tumor circumference.

(C) Hematoxylin and eosin staining of sections of tumors from mice treated with vehicle or 40 mg/kg MLN8054 at day 3 (high-magnification views are shown on the right). Black arrows (top row) indicate neuronal differentiation with the presence of variably maturing ganglion-like cells. Green arrows (middle row) indicate mitotic cells. Orange arrows (bottom row) show a multivacuolated histiocytic component around tumors. Scale bars represent 50 μm (left and middle) or 10 μm (right).

(D) Immunohistochemistry of tumors treated as (A), using indicated antibodies. Scale bar represents 50 μm.

(E) Kaplan-Meier plot documenting survival of mice treated twice daily with 15 mg/kg MLN8054 versus vehicle.

(F) Kaplan-Meier plot documenting survival of mice treated with 30 mg/kg MLN8237 versus vehicle.

See also Figure S6.

Gene Expression Analyses

Total RNA was reverse transcribed into complementary DNA (cDNA) using random hexanucleotide primers and M-MLV reverse transcriptase. Quantitative RT-PCR was performed in triplicates with cDNA corresponding to 40 ng total RNA using Absolute QPCR SYBR Green mix (ABgene) on the Mx3000P system (Stratagene) at a 60°C annealing temperature. Relative expression was calculated according to the ΔΔCt relative quantification method using the average expression of *RPS14* and *B2M* as calibrator. Primers are listed in Supplemental Experimental Procedures.

In Situ Proximity Ligation Assay

Duolink in situ proximity ligation assay (PLA; Olink Bioscience) was performed on fixed adherent cells according to the manufacturer's instructions. Briefly, SH-EP neuroblastomas cells expressing N-Myc were fixed in 4% paraformaldehyde for 30 min, permeabilized with 0.2% Triton X-100, and blocked with the manufacturer's blocking agent for 1 hr followed by incubation with paired primary antibodies, N-Myc (Calbiochem) with Aurora-A (Cell Signaling) or Max (Cell Signaling), for 1 hr. PLA detection was performed as recommended by the manufacturer. Images were taken and analyzed using the InCell Analyzer 1000 (Plan 20× objective).

Additional experimental procedures can be found in Supplemental Information.

ACCESSION NUMBERS

All microarray data have been deposited in the ArrayExpress database (http://www.ebi.ac.uk/arrayexpress) under accession number E-MTAB-179.

SUPPLEMENTAL INFORMATION

Supplemental Information includes Supplemental Experimental Procedures and six figures and can be found with this article online at http://dx.doi.org/10.1016/j.ccr.2013.05.005.

ACKNOWLEDGMENTS

We thank Hermann Schindelin and Richard Bayliss for their advice on analyzing the MLN8054/Aurora-A interaction. This study was supported by grants from the Federal Ministry of Education and Research ("NGFN plus"; to M.E., H.E.D., and O.W.), the Christopher's Smile Project (grant CSM001X), SPARKS (grant 09RMH01), The Neuroblastoma Society (grant NES003X), and the Medical Research Council (MRC; grant NC3R-G1000121/94513 to L.C.). We also acknowledge The Institute of Cancer Research CR-UK and EPSRC Cancer Imaging Centre, in association with the MRC and Department of Health (England) grant C1060/A10334 (to S.R.), NHS funding to the NIHR Biomedical Research Centre, and The Wellcome Trust (grant 091763Z/10/Z; to S.R.). We thank Florence Raynaud, Amin Mirza, Albert Hallsworth, Zai Ahmad, and Karen Barker for guidance with in vivo studies and members of the Eilers and Chesler laboratories for their critical reading of and comments on the manuscript.

Received: May 17, 2012
Revised: April 21, 2013
Accepted: May 8, 2013
Published: June 20, 2013

REFERENCES

Beltran, H., Rickman, D.S., Park, K., Chae, S.S., Sboner, A., MacDonald, T.Y., Wang, Y., Sheikh, K.L., Terry, S., Tagawa, S.T., et al. (2011). Molecular characterization of neuroendocrine prostate cancer and identification of new drug targets. Cancer Discov. *1*, 487–495.

Bouchard, C., Dittrich, O., Kiermaier, A., Dohmann, K., Menkel, A., Eilers, M., and Lüscher, B. (2001). Regulation of cyclin D2 gene expression by the Myc/Max/Mad network: Myc-dependent TRRAP recruitment and histone acetylation at the cyclin D2 promoter. Genes Dev. *15*, 2042–2047.

Brodeur, G.M., Seeger, R.C., Schwab, M., Varmus, H.E., and Bishop, J.M. (1984). Amplification of N-*myc* in untreated human neuroblastomas correlates with advanced disease stage. Science *224*, 1121–1124.

Bruggeman, S.W., Valk-Lingbeek, M.E., van der Stoop, P.P., Jacobs, J.J., Kieboom, K., Tanger, E., Hulsman, D., Leung, C., Arsenijevic, Y., Marino, S., and van Lohuizen, M. (2005). Ink4a and Arf differentially affect cell proliferation and neural stem cell self-renewal in Bmi1-deficient mice. Genes Dev. *19*, 1438–1443.

Chanthery, Y.H., Gustafson, W.C., Itsara, M., Persson, A., Hackett, C.S., Grimmer, M., Charron, E., Yakovenko, S., Kim, G., Matthay, K.K., and Weiss, W.A. (2012). Paracrine signaling through MYCN enhances tumor-vascular interactions in neuroblastoma. Science translational medicine *4*, 115ra113.

Chen, X., Xu, H., Yuan, P., Fang, F., Huss, M., Vega, V.B., Wong, E., Orlov, Y.L., Zhang, W., Jiang, J., et al. (2008). Integration of external signaling pathways with the core transcriptional network in embryonic stem cells. Cell *133*, 1106–1117.

Delmore, J.E., Issa, G.C., Lemieux, M.E., Rahl, P.B., Shi, J., Jacobs, H.M., Kastritis, E., Gilpatrick, T., Paranal, R.M., Qi, J., et al. (2011). BET bromodomain inhibition as a therapeutic strategy to target c-Myc. Cell *146*, 904–917.

Dodson, C.A., Kosmopoulou, M., Richards, M.W., Atrash, B., Bavetsias, V., Blagg, J., and Bayliss, R. (2010). Crystal structure of an Aurora-A mutant that mimics Aurora-B bound to MLN8054: insights into selectivity and drug design. Biochem. J. *427*, 19–28.

Faisal, A., Vaughan, L., Bavetsias, V., Sun, C., Atrash, B., Avery, S., Jamin, Y., Robinson, S.P., Workman, P., Blagg, J., et al. (2011). The aurora kinase inhibitor CCT137690 downregulates MYCN and sensitizes MYCN-amplified neuroblastoma in vivo. Mol. Cancer Ther. *10*, 2115–2123.

Gullberg, M., Fredriksson, S., Taussig, M., Jarvius, J., Gustafsdottir, S., and Landegren, U. (2003). A sense of closeness: protein detection by proximity ligation. Curr. Opin. Biotechnol. *14*, 82–86.

Hatton, B.A., Knoepfler, P.S., Kenney, A.M., Rowitch, D.H., de Alborán, I.M., Olson, J.M., and Eisenman, R.N. (2006). N-myc is an essential downstream effector of Shh signaling during both normal and neoplastic cerebellar growth. Cancer Res. *66*, 8655–8661.

Herold, S., Wanzel, M., Beuger, V., Frohme, C., Beul, D., Hillukkala, T., Syvaoja, J., Saluz, H.P., Haenel, F., and Eilers, M. (2002). Negative regulation of the mammalian UV response by Myc through association with Miz-1. Mol. Cell *10*, 509–521.

Horn, V., Thélu, J., Garcia, A., Albigès-Rizo, C., Block, M.R., and Viallet, J. (2007). Functional interaction of Aurora-A and PP2A during mitosis. Mol. Biol. Cell *18*, 1233–1241.

Kawauchi, D., Robinson, G., Uziel, T., Gibson, P., Rehg, J., Gao, C., Finkelstein, D., Qu, C., Pounds, S., Ellison, D.W., et al. (2012). A mouse model of the most aggressive subgroup of human medulloblastoma. Cancer Cell *21*, 168–180.

Kim, Y.H., Girard, L., Giacomini, C.P., Wang, P., Hernandez-Boussard, T., Tibshirani, R., Minna, J.D., and Pollack, J.R. (2006). Combined microarray analysis of small cell lung cancer reveals altered apoptotic balance and distinct expression signatures of MYC family gene amplification. Oncogene *25*, 130–138.

Manfredi, M.G., Ecsedy, J.A., Meetze, K.A., Balani, S.K., Burenkova, O., Chen, W., Galvin, K.M., Hoar, K.M., Huck, J.J., LeRoy, P.J., et al. (2007). Antitumor activity of MLN8054, an orally active small-molecule inhibitor of Aurora A kinase. Proc. Natl. Acad. Sci. USA *104*, 4106–4111.

Manfredi, M.G., Ecsedy, J.A., Chakravarty, A., Silverman, L., Zhang, M., Hoar, K.M., Stroud, S.G., Chen, W., Shinde, V., Huck, J.J., et al. (2011). Characterization of Alisertib (MLN8237), an investigational small-molecule inhibitor of aurora A kinase using novel in vivo pharmacodynamic assays. Clin. Cancer Res. *17*, 7614–7624.

Marumoto, T., Zhang, D., and Saya, H. (2005). Aurora-A - a guardian of poles. Nat. Rev. Cancer *5*, 42–50.

Matulonis, U.A., Sharma, S., Ghamande, S., Gordon, M.S., Del Prete, S.A., Ray-Coquard, I., Kutarska, E., Liu, H., Fingert, H., Zhou, X., et al. (2012).

Phase II study of MLN8237 (alisertib), an investigational Aurora A kinase inhibitor, in patients with platinum-resistant or -refractory epithelial ovarian, fallopian tube, or primary peritoneal carcinoma. Gynecol. Oncol. *127*, 63–69.

Miliani de Marval, P.L., Macias, E., Rounbehler, R., Sicinski, P., Kiyokawa, H., Johnson, D.G., Conti, C.J., and Rodriguez-Puebla, M.L. (2004). Lack of cyclin-dependent kinase 4 inhibits c-myc tumorigenic activities in epithelial tissues. Mol. Cell. Biol. *24*, 7538–7547.

Nilsson, J.A., Keller, U.B., Baudino, T.A., Yang, C., Norton, S., Old, J.A., Nilsson, L.M., Neale, G., Kramer, D.L., Porter, C.W., and Cleveland, J.L. (2005). Targeting ornithine decarboxylase in Myc-induced lymphomagenesis prevents tumor formation. Cancer Cell *7*, 433–444.

Oberthuer, A., Hero, B., Berthold, F., Juraeva, D., Faldum, A., Kahlert, Y., Asgharzadeh, S., Seeger, R., Scaruffi, P., Tonini, G.P., et al. (2010). Prognostic impact of gene expression-based classification for neuroblastoma. J. Clin. Oncol. *28*, 3506–3515.

Otto, T., Horn, S., Brockmann, M., Eilers, U., Schüttrumpf, L., Popov, N., Kenney, A.M., Schulte, J.H., Beijersbergen, R., Christiansen, H., et al. (2009). Stabilization of N-Myc is a critical function of Aurora A in human neuroblastoma. Cancer Cell *15*, 67–78.

Popov, N., Wanzel, M., Madiredjo, M., Zhang, D., Beijersbergen, R., Bernards, R., Moll, R., Elledge, S.J., and Eilers, M. (2007). The ubiquitin-specific protease USP28 is required for MYC stability. Nat. Cell Biol. *9*, 765–774.

Rakhra, K., Bachireddy, P., Zabuawala, T., Zeiser, R., Xu, L., Kopelman, A., Fan, A.C., Yang, Q., Braunstein, L., Crosby, E., et al. (2010). CD4(+) T cells contribute to the remodeling of the microenvironment required for sustained tumor regression upon oncogene inactivation. Cancer Cell *18*, 485–498.

Seki, A., Coppinger, J.A., Jang, C.Y., Yates, J.R., and Fang, G. (2008). Bora and the kinase Aurora a cooperatively activate the kinase Plk1 and control mitotic entry. Science *320*, 1655–1658.

Shang, X., Burlingame, S.M., Okcu, M.F., Ge, N., Russell, H.V., Egler, R.A., David, R.D., Vasudevan, S.A., Yang, J., and Nuchtern, J.G. (2009). Aurora A is a negative prognostic factor and a new therapeutic target in human neuroblastoma. Mol. Cancer Ther. *8*, 2461–2469.

Shimomura, T., Hasako, S., Nakatsuru, Y., Mita, T., Ichikawa, K., Kodera, T., Sakai, T., Nambu, T., Miyamoto, M., Takahashi, I., et al. (2010). MK-5108, a highly selective Aurora-A kinase inhibitor, shows antitumor activity alone and in combination with docetaxel. Mol. Cancer Ther. *9*, 157–166.

Sjostrom, S.K., Finn, G., Hahn, W.C., Rowitch, D.H., and Kenney, A.M. (2005). The Cdk1 complex plays a prime role in regulating N-myc phosphorylation and turnover in neural precursors. Dev. Cell *9*, 327–338.

Sloane, D.A., Trikic, M.Z., Chu, M.L., Lamers, M.B., Mason, C.S., Mueller, I., Savory, W.J., Williams, D.H., and Eyers, P.A. (2010). Drug-resistant aurora A mutants for cellular target validation of the small molecule kinase inhibitors MLN8054 and MLN8237. ACS Chem. Biol. *5*, 563–576.

Sodir, N.M., Swigart, L.B., Karnezis, A.N., Hanahan, D., Evan, G.I., and Soucek, L. (2011). Endogenous Myc maintains the tumor microenvironment. Genes Dev. *25*, 907–916.

Subramanian, A., Tamayo, P., Mootha, V.K., Mukherjee, S., Ebert, B.L., Gillette, M.A., Paulovich, A., Pomeroy, S.L., Golub, T.R., Lander, E.S., and Mesirov, J.P. (2005). Gene set enrichment analysis: a knowledge-based approach for interpreting genome-wide expression profiles. Proc. Natl. Acad. Sci. USA *102*, 15545–15550.

Valentijn, L.J., Koster, J., Haneveld, F., Aissa, R.A., van Sluis, P., Broekmans, M.E., Molenaar, J.J., van Nes, J., and Versteeg, R. (2012). Functional MYCN signature predicts outcome of neuroblastoma irrespective of MYCN amplification. Proc. Natl. Acad. Sci. USA *109*, 19190–19195.

Weiss, W.A., Aldape, K., Mohapatra, G., Feuerstein, B.G., and Bishop, J.M. (1997). Targeted expression of MYCN causes neuroblastoma in transgenic mice. EMBO J. *16*, 2985–2995.

Welcker, M., Orian, A., Jin, J., Grim, J.E., Harper, J.W., Eisenman, R.N., and Clurman, B.E. (2004). The Fbw7 tumor suppressor regulates glycogen synthase kinase 3 phosphorylation-dependent c-Myc protein degradation. Proc. Natl. Acad. Sci. USA *101*, 9085–9090.

Wenzel, A., Cziepluch, C., Hamann, U., Schürmann, J., and Schwab, M. (1991). The N-Myc oncoprotein is associated in vivo with the phosphoprotein Max(p20/22) in human neuroblastoma cells. EMBO J. *10*, 3703–3712.

Wong, D.J., Liu, H., Ridky, T.W., Cassarino, D., Segal, E., and Chang, H.Y. (2008). Module map of stem cell genes guides creation of epithelial cancer stem cells. Cell Stem Cell *2*, 333–344.

Workman, P., Aboagye, E.O., Balkwill, F., Balmain, A., Bruder, G., Chaplin, D.J., Double, J.A., Everitt, J., Farningham, D.A., Glennie, M.J., et al.; Committee of the National Cancer Research Institute. (2010). Guidelines for the welfare and use of animals in cancer research. Br. J. Cancer *102*, 1555–1577.

Yada, M., Hatakeyama, S., Kamura, T., Nishiyama, M., Tsunematsu, R., Imaki, H., Ishida, N., Okumura, F., Nakayama, K., and Nakayama, K.I. (2004). Phosphorylation-dependent degradation of c-Myc is mediated by the F-box protein Fbw7. EMBO J. *23*, 2116–2125.

Yeh, E., Cunningham, M., Arnold, H., Chasse, D., Monteith, T., Ivaldi, G., Hahn, W.C., Stukenberg, P.T., Shenolikar, S., Uchida, T., et al. (2004). A signalling pathway controlling c-Myc degradation that impacts oncogenic transformation of human cells. Nat. Cell Biol. *6*, 308–318.